Journal of Electrical Engineering & Technology, Vol. 1, No. 2, pp. 185~191, 2006 **185**

A Novel Stator Hybrid Excited Doubly Salient Permanent Magnet Brushless Machine for Electric Vehicles

Xiaoyong Zhu* and Ming Cheng**

Abstract - In this paper, a novel stator hybrid excited doubly salient permanent magnet (SHEDS-PM) brushless machine with a special magnetic bridge is proposed for the first time. The originality of this machine is purposely to add a magnetic bridge in shunt with each PM pole, which not only maintains the stator lamination in its entireness, but also amplifies the effect of DC field flux on PM flux. An equivalent magnetic circuit is presented to clarify the novelty. Based on the 2-D finite element analysis, the static characteristics of the SHEDS-PM machine, namely phase flux linkage, back-EMF, cogging torque, winding inductance and static torque are deduced. The corresponding results on a prototype machine illustrate that the proposed machine is promising for application to electric vehicles.

Keywords: hybrid excited, doubly salient machine, permanent magnet (PM) machine, finite element analysis (FEA)

1. Introduction

Demand for more compact, efficient and cheaper electric machines has grown tremendously during the last decade. Meanwhile, a great progress has been achieved not only in the development of permanent magnets but also in the area of electric machine design and power electronics as well. Therefore, PM machines have been drawing more and more attention [1].

However, as is well known, flux control capability of PM machines is much more difficult to achieve than that in electric machines with DC excitation [2]. Air-gap flux control of PM machines can generally be accomplished by two means: control techniques and suitable modification of the machine topology. Conventional PM machines have a fixed magnet excitation which limits the drive's capability and becomes a significant limitation. The machines are operated at constant volt/hertz operation up to the base speed and constant voltage operation which requires weakening of the field at higher speeds to extend the speed range. Above the base speed, vector control techniques are typically used to weaken the air-gap flux. However, these techniques cause large demagnetization current to flow in the machine d-axis and results in high copper losses and demagnetization risk of the magnets. Furthermore, the magnets may be forced to operate in the irreversible demagnetization region, which could permanently demagnetize the magnets by not allowing the magnet to return to its original operating point even after the current is removed.

How to realize field weakening in PM machines without demagnetizing permanent magnets is always of great interest as well as challenging to both PM machine designers and control engineers. Recently, there is an increasing tendency to study hybrid excitation machines, which combine the advantages of PM machines with the possibility of controllable magnetic flux by auxiliary DC windings [3]. The initial research has revealed that the hybrid excitation permanent magnet (HEPM) machines can offer the advantages of high power density, high efficiency and robust rotor structure. Moreover, the most attractive performance is its special ability of the flux weakening in the operation of constant power, which is very important for electric vehicles (EV).

In this paper, a novel stator hybrid excited doubly salient permanent magnet (SHEDS-PM) brushless machine with a special magnetic bridge is proposed for the first time. The operation principle of the SHEDS-PM machine is described. A 12/8-pole HEDS motor has been designed and built for evaluation. An equivalent magnetic circuit model is presented to clarify the function of the retained magnetic bridge. In addition, the capability of flux control is obtained based on the nonlinear finite element analysis (FEA). Experimental results of the prototype machine are given to verify the theoretical analysis.

2. Machine Topology and Operation Principle

Fig. 1 shows the proposed motor topology, which is a three-phase 12/8-pole machine. It consists of two types of stator windings, a three-phase armature winding and a DC

---

* Department of Electrical Engineering, Southeast University, P.R. China. (zxyff@ujs.edu.cn)

** School of Electrical and Information Engineering, Jiangsu University, P.R. China. (mcheng@seu.edu.cn)

Received February 18, 2006 ; Accepted April 17, 2006

excitation winding. The function of the armature winding is the same as that for a DSPM machine [4]-[5], whereas the DC field winding not only works as an electromagnet but also as a tool for flux weakening and efficiency optimization. Notice that flux weakening operation is necessary for high-speed EV cursing, whereas efficiency optimizing control is essential for long EV driving range [6]. The originality of this topology is to purposely add an extra flux path in shunt with each PM pole, the so-called magnetic bridge. This magnetic bridge not only maintains the stator lamination in its entireness, but also amplifies the effect of DC field flux on PM flux.

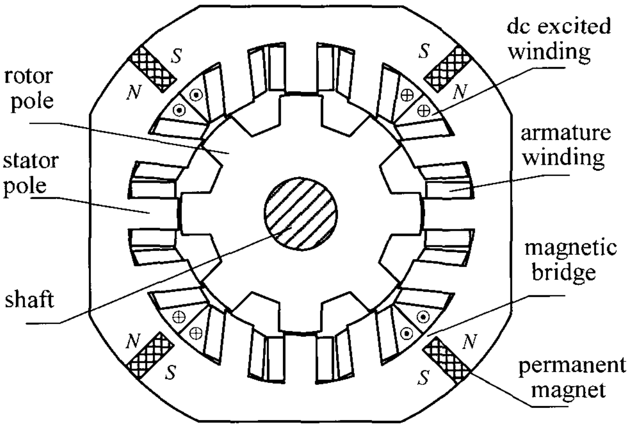

Fig. 1 Cross-section of the SHEDS-PM machine

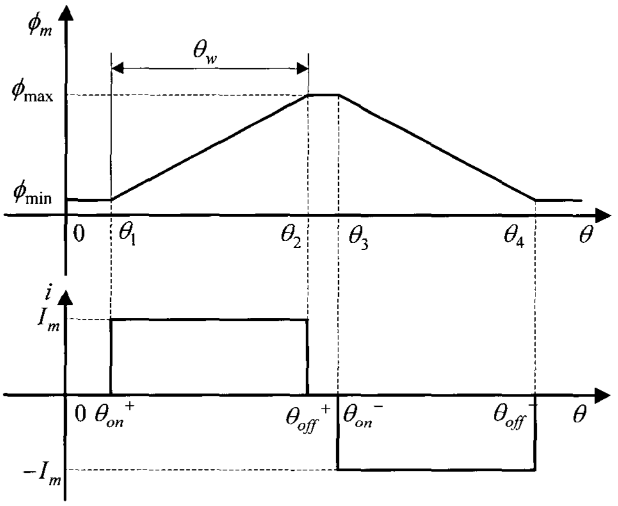

Fig. 2 Theoretical flux and current waveforms

The theoretical waveforms of PM flux ϕ_m and phase current i with respect to the rotor position are shown in Fig. 2. From Fig. 3, when a rotor pole is entering the region occupied by a conductive phase, the flux is increasing. If a positive current is applied to the winding, a positive torque will be produced. When the rotor pole is leaving the stator pole from the aligned position, the flux is decreasing and also a positive torque will be produced if a negative current is applied to the winding. Thus, two possible torque producing zones are fully utilized [7].

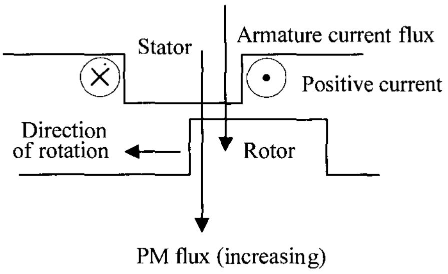

(a) Rotor reaches stator and phase current is positive

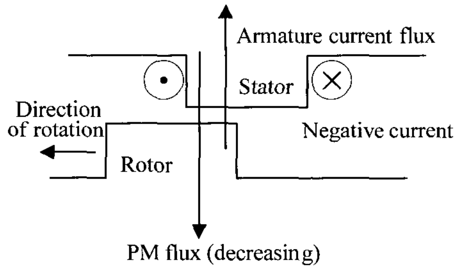

(b) Rotor leaves stator and phase current is negative

Fig. 3 Flux direction for the HEDS motor

3. Magnetic Circuit Analysis

As mentioned, the novelty of the proposed machine topology is to purposely retain an extra flux path in shunt with each PM pole. In order to illustrate its merit and to clarify how the magnetic bridge amplifies the effect of DC flux on PM flux, an equivalent magnetic circuit model is presented for analysis.

Fig. 4 (a) shows the equivalent magnetic circuit of the machine with magnetic bridge, and Fig. 4 (b) illustrates the circuit of the machine without magnetic bridge at no-load.

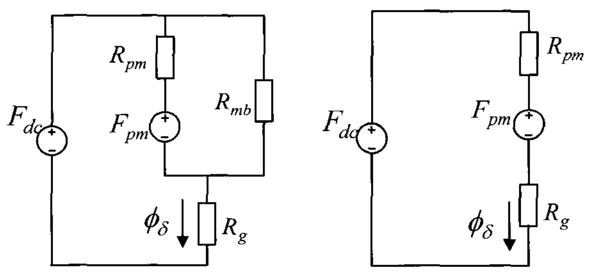

(a) With a magnetic bridge (b) Without magnetic bridge

Fig. 4 Equivalent magnetic circuits at no load

In Fig. 4 (a), the air gap flux ϕ_δ can be expressed as:

$$\phi_\delta = \frac{F_{dc}(R_{mb}+R_{pm})+F_{pm}R_{mb}}{R_{mb}R_g+R_{pm}R_g+R_{mb}R_{pm}} \tag{1}$$

When the DC current is set to zero, namely $F_{dc}=0$, the corresponding flux is given by:

$$\phi_{\delta 0}=\frac{F_{pm}R_{mb}}{R_{mb}R_g+R_{pm}R_g+R_{mb}R_{pm}} \tag{2}$$

where F_{dc} is the magnetic motive force (MMF) of DC current excitation, F_{pm} is the PM excitation. R_{pm} is the reluctance of the PM pole. R_{mb} is the reluctance of the extra magnetic bridge, and R_g is the reluctance of the air-gap.

When a positive DC field current is applied, $F_{dc}=F_{dc+}$, the corresponding air-gap flux can be expressed as:

$$\phi_{\delta +}=\frac{F_{dc+}(R_{mb}+R_{pm})+F_{pm}R_{mb}}{R_{mb}R_g+R_{pm}R_g+R_{mb}R_{pm}} \tag{3}$$

When a negative DC field current is applied, $F_{dc}=F_{dc-}$ the corresponding air-gap flux is given by:

$$\phi_{\delta -}=\frac{F_{dc-}(R_{mb}+R_{pm})+F_{pm}R_{mb}}{R_{mb}R_g+R_{pm}R_g+R_{mb}R_{pm}} \tag{4}$$

With (2), (3) and (4), it yields:

$$F_{dc+}=\frac{\dfrac{\phi_{\delta +}}{\phi_{\delta 0}}-1}{\dfrac{R_{pm}}{R_{mb}}+1}F_{pm} \tag{5}$$

$$F_{dc-}=\frac{1-\dfrac{\phi_{\delta +}}{\phi_{\delta 0}}}{\dfrac{R_{pm}}{R_{mb}}+1}F_{pm} \tag{6}$$

Similar results can be derived from Fig.4 (b) where there is no magnetic bridge, namely R_{mb} is set to infinite:

$$F'_{dc+}=(\frac{\phi_{\delta +}}{\phi_{\delta 0}}-1)F_{pm} \tag{7}$$

$$F'_{dc-}=(1-\frac{\phi_{\delta -}}{\phi_{\delta 0}})F_{pm} \tag{8}$$

If $\phi_{\delta +}/\phi_{\delta 0}=2$ and $\phi_{\delta -}/\phi_{\delta 0}=1/2$ are wanted, the MMF of DC excitation can be derived as following when selecting $R_{mb}/R_{pm}=1/3$:

$$\left.\begin{aligned}F_{dc+}&=F_{pm}/4\\ F_{dc-}&=F_{pm}/8\end{aligned}\right\} \tag{9}$$

Similarly, the DC excitation required to achieve the same flux variation without magnetic bridge can also be obtained as:

$$\left.\begin{aligned}F'_{dc+}&=F_{pm}\\ F'_{dc-}&=F_{pm}/2\end{aligned}\right\} \tag{10}$$

Comparing (9) with (10) illustrates that, for the machine with magnetic bridge, $\phi_{\delta +}/\phi_{\delta -}=4$ only needs a small change in DC excitation, namely 25% of F_{pm} during flux strengthening, and 12.5% of F_{pm} during flux weakening, whereas 100% and 50% of F_{pm} are needed in DC excitation of the machine without magnetic bridge.

Therefore the conclusion can be drawn that because of the special machine topology arrangement with magnetic bridge, the reluctance of the extra DC flux path is fairly low so that the required DC ampere turns are comparatively small. That is to say, this magnetic bridge not only maintains the stator lamination in its entireness, but also amplifies the effect of DC flux on PM flux.

Table 1 Design data of 12/8-Pole SHEDS-PM motor

Rated Power (W)	750
Rated speed (r/min)	1500
DC bus voltage (V)	95
Stator inner diameter (mm)	75
Stack length (mm)	75
Air-gap length (mm)	0.35
Stator pole arc (degree)	15
Rotor pole arc (degree)	20
Number of turns/phase	120
DC field windings turns	200
Magnet volume (mm^3)	4×(4.5×18.5×75)

4. Magnetic Field Analysis and Static Characteristics

The performance of the motor, whose main design parameters are given in Table 1, is predicted by using 2-D nonlinear finite element analysis. In order to assess the performance of the proposed machine more accurate, its iron core and magnetic saturation, leakage flux and armature reaction are taken into account.

4.1 The Flux Distribution

Fig. 5 shows the flux distributions of the proposed machine at θ=0° for three different cases of the DC field current (0 A-turns, +600 A-turns and -600 A-turns). When the DC excitation MMF reinforces the PM MMF, this extra flux path will assist the effect of flux strengthening. On the other hand, if the DC field MMF opposes the PM MMF, this extra flux path will weaken the PM flux leakage.

To scale the grade of the field control range, a flux control factor α can be defined as follows:

$$\alpha = (B_\delta - B_{\delta 0}) / B_{\delta 0} \times 100\% \tag{11}$$

where $B_{\delta 0}$ is the flux density of the air-gap without DC field current, B_δ is the flux density when the DC field current is applied. Fig. 6 shows the field control range with and without magnetic bridge respectively.

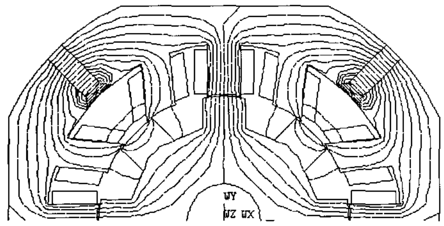

(a) PMs only

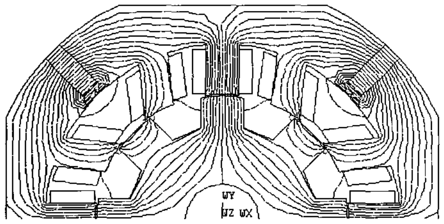

(b) PMs and F_{dc}=600 A-turns

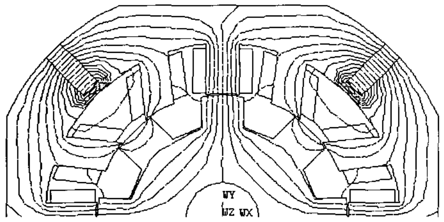

(c) PMs and F_{dc}=-600 A-turns

Fig. 5 Flux distributions of different DC excitations at θ=0°

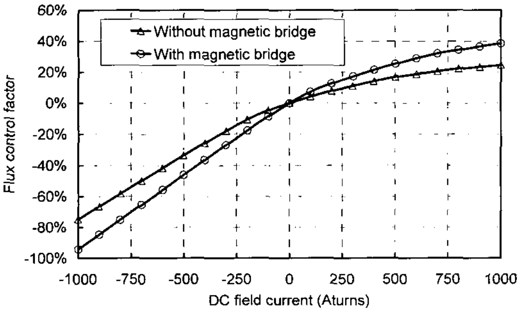

Fig. 6 The capability of flux control with and without magnetic bridge

4.2 PM Flux Linkage and Back EMF

When the machine operates at a constant speed with no-load, the corresponding flux linkages with respect to the rotor position for three different cases of the DC field current (0 A-turns, +600 A-turns and -600 A-turns) are simulated as shown in Fig. 7.

Comparing Fig. 7 (a) with Fig. 7(b) shows that due to the reluctance of the extra path is much less than that of PMs without magnetic bridge, the existence of magnetic bridge amplifies the effect of flux weakening, which agrees with the previous results from magnetic circuit analysis.

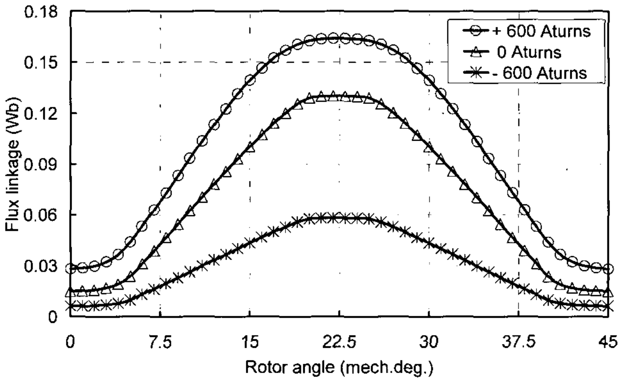

(a) With magnetic bridge

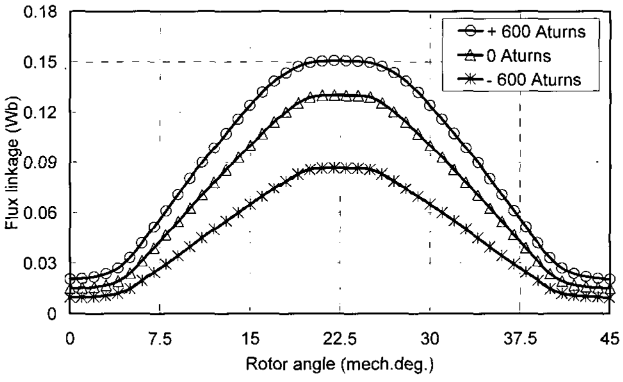

(b) Without magnetic bridges

Fig. 7 Flux linkages at different dc excitation currents

The phase back-EMF can be determined from:

$$e = -\frac{d\psi}{dt} = -\omega \frac{d\psi}{d\theta} \tag{12}$$

where ψ is the phase flux-linkage, ω is rotor speed in rad/s, and θ is the rotor angle in radians. Fig. 8 shows the predicted and measured back EMF waveforms of the 12/8-pole prototype respectively. From Fig. 8, the motor still retains the desired trapezoidal back-EMF waveform, which means the proposed motor is more suitable for BLDC operation.

4.3 Inductances

In the calculation of inductances, the cross-coupling between the PM flux, armature flux and DC excitation flux should be taken into account. As the PM, armature current and DC excitation current act together, the flux linkage of one phase is given by:

$$\psi = \psi_{pm} + L_a i_a + L_{af} i_f \tag{13}$$

When keeping the dc excitation current i_f constant, the armature current $+i_a$ and $-i_a$ are applied respectively, the flux linkage of one phase is:

$$\psi_+ = \psi_{pm} + L_a i_a + L_{af} i_f \tag{14}$$

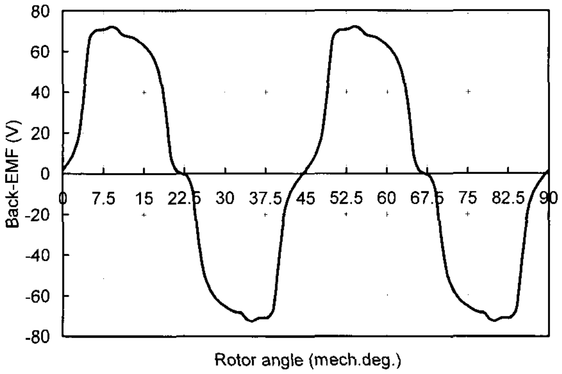

(a) Predicted

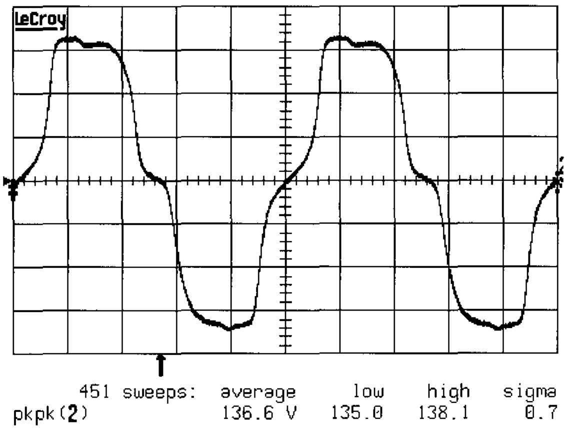

(b) Measured

Fig. 8 Back-EMF waveforms at 1500 r/min

$$\psi_- = \psi_{pm} - L_a i_a + L_{af} i_f \tag{15}$$

Then, the self-inductance can be derived from (13) and (14) as:

$$L_a = \frac{\psi_+ - \psi_-}{2 i_a} \tag{16}$$

Similarly, when keeping $i_a = 0$, the mutual inductance is given by:

$$L_{af} = \frac{\psi - \psi_{pm}}{i_f} \tag{17}$$

where L_a is the self-inductance of Phase A, L_{af} the mutual inductance between Phase A and field winding, ψ_{pm} the PM flux-linkage.

The self-inductance and mutual inductance characteristics are shown in Fig. 9 and Fig. 10, respectively.

4.4 Static Torque

Based on the resulted PM flux linkage and inductance, the electromagnetic static torque for one-phase-on condition can be deduced by using the co-energy method as:

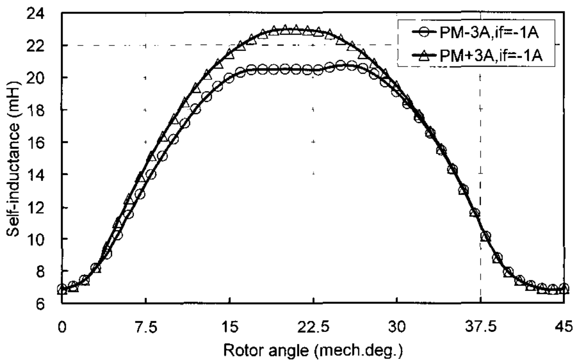

Fig. 9 Phase self-inductance versus rotor angle

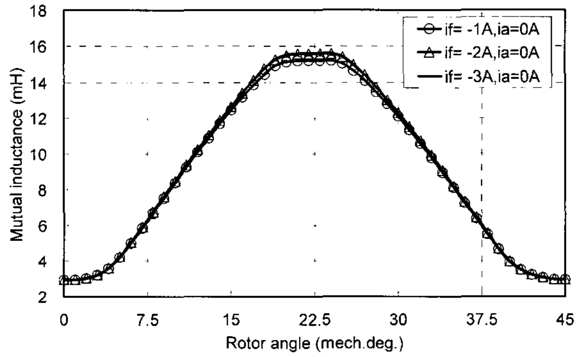

Fig. 10 Mutual inductance between dc excited windings and the armature windings

$$\begin{aligned} T_e &= \frac{\partial W'(i_a, i_f, \theta)}{\partial \theta} \\ &= i_a \frac{d\psi_{PM}}{d\theta} + \frac{1}{2} i_a^2 \frac{dL_a}{d\theta} + i_a i_f \frac{dL_{af}}{d\theta} - \frac{dW_{PM}}{d\theta} \\ &= T_{PM} + T_r + T_f - T_{cog} \end{aligned} \tag{18}$$

where T_{PM} is the reaction torque due to the interaction between PM fluxes and winding current, T_r is the reluctance torque due to the variation of the inductance, T_f is the DC excitation torque and T_{cog} is the cogging torque.

Fig. 11 shows the total electromagnetic static torque and its components when $i_a = \pm 3$ A and $i_f = -1$ A.

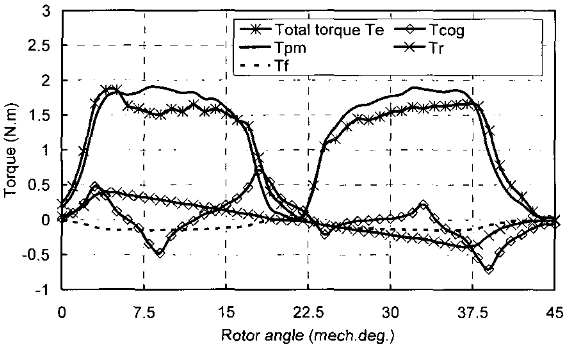

Fig. 11 Total torque and its components

It is seen from Fig. 11 that the average of reluctance torque is near zero and contributes little to the total electromagnetic torque but causes torque ripple. The permanent magnet torque is dominant component in the SHEDS-PM motor. In addition, the significant cogging torque component is found, which causes also torque ripple. Hence, some measures such as rotor skewing may be adopted to minimize the torque ripple.

5. Conclusions

This paper proposes a novel stator hybrid excited doubly salient permanent magnet brushless motor. An equivalent magnetic circuit of the machine has been presented, which reveals the advantages of the machine. The finite element analysis has been carried out. Based on the parameters resulting from the FEA, the static characteristics, namely inductances, flux linkage, back EMF and torque, are deduced. Based on the theoretical study in SHEDS-PM machine by using 2-D FEA and the equivalent magnetic circuit, the following conclusions may be drawn:

The novelty of this machine is addition of an extra flux path in shunt with each PM pole, hence amplifying the effect of flux weakening for constant power operation. Thus, the proposed machine not only offers the advantages of a DSPM machine, but also a very wide speed range that is essential for EV application.

The hybrid excitation machine provides an additional degree of freedom with respect to the flux weakening method by means of armature current control alone. It also allows to avoid the constraints and drawbacks associated with the armature current vector control method and to widen the speed range at constant-power operation mode.

Acknowledgements

This work was supported by grants from NSFC (Project No.: 50337030, 50377004).

References

[1] T. A. Lipo and M. Aydin, "Field weakening of permanent magnet machines - design approaches," EPE Power Electronics and Motion Control Conference, Riga, Latvia, pp. 1-6, Sept. 2004.

[2] M. Aydin, Surong Huang and T.A. Lipo, "A new axial flux surface mounted permanent magnet machine capable of field control," *Proc. of 37th IAS Annual Meeting*, pp. 1250-1257, 2002.

[3] X. Zhu and M. Cheng, "An overview of hybrid excitation permanent magnet machines," *Proc. ICEMS, Jeju, Korea, Nov. 1-3,* CD-ROM, pp. 1-4, 2004.

[4] M. Cheng, K.T. Chau and C.C. Chan, "Design and analysis of a new doubly salient permanent magnet motor", *IEEE Trans. Magnetics*, vol. 37, no. 4, pp. 3012-3020, 2001.

[5] M. Cheng, K.T. Chau, C.C. Chan and Q. Sun, "Control and operation of a new 8/6-pole doubly salient permanent magnet motor drive", *IEEE Transactions on Industry Applications,* vol. 39, no. 5, pp. 1363-1371, 2003.

[6] C.C. Chan and K.T. Chau, *Modern Electric Vehicle Technology*, London: Oxford University Press, 2001.

[7] M. Cheng and E. Zhou, "Analysis and control of a novel split-winding doubly salient permanent magnet motor for adjustable speed drive", *Science in China (Series E),* vol. 44, no. 4, pp. 353-364, 2001.

Xiaoyong Zhu
He received the B. Sc. degree in electrical automation in 1997 and the M. Sc. degree in electrical engineering in 2002 from Jiangsu University, Zhenjiang, P. R. China. He is currently working toward the Ph.D. degree in Southeast University. His areas of interest include electrical machines and drives, intelligent control, and power electronics.

Ming Cheng
He received the B.Sc. and M.Sc. degrees in electrical engineering from Southeast University in 1982 and 1987, respectively, and Ph.D. degree in electrical and electronic engineering from The University of Hong Kong in 2001.

Since 1987, he has been with Southeast University, where he is currently the Head and a Professor in the Department of Electrical Engineering. His areas of interests include electrical machines, motor drives and power electronics. He has authored over 80 technical papers and holds 7 patents in these areas. He has also served as the Chair and/or an organizing committee member for many international conferences.